Surface stress and reversing size effect in the initial yielding of ultrathin films[1]

G. Gioia and X. Dai
Department of Theoretical and Applied Mechanics
University of Illinois, Urbana, Il 61801

Very recent experiments indicate that in free-standing metallic films of constant grain size the initial yield stress increases as the film becomes thinner, it peaks for a thickness on the order of 100 nm, and then starts to decrease. This reversing size effect poses two challenges: (1) It cannot be explained using currently available models and (2) it appears to contradict the classical experimental results due to J. W. Beams. Here we show that the reversing size effect can be explained and the contradiction dispelled by taking into account how the initial yielding is affected by the surface stress. We also predict that the mode of failure of a film changes from ductile to brittle for a thickness on the order of 100 nm, in accord with experiments.

1 Introduction

The mechanical behavior of tiny metallic bodies has long been known to be subject to size effects [1]. For example, the yield stress of crystalline whiskers may exceed the yield stress of large crystals of the same material by a factor of 10 or more [2]. With the development of nanotechnologies in recent years, much new research has been devoted to elucidating size effects in polycrystalline ultrathin films.

[1]To appear in Journal of Applied Mechanics, 2005

One size effect that has drawn much attention pertains to the large strain gradients that arise, for example, in films subjected to bending. This size effect has been ascribed to the high density of geometrically necessary dislocations induced by the strain gradient [3, 4]. Another size effect pertains to the texture (or preferential grain orientation) that is characteristic of thin films grown on crystalline substrates. Because a texture frequently leads to a higher yield stress [5, 6], this size effect can be readily explained. Still another size effect pertains to the grain size, which in annealed films tends to scale with the thickness of the film [5, 6]. Because smaller grains lead to a higher yield stress (the Hall–Petch relation [7, 8, 9]) or perhaps to a lower yield stress (the reverse Hall–Petch relation, valid for grains smaller than about 10 nm [10]), this size effect can be readily explained.

In a very recent experimental study [11], the yield stress of gold films of constant texture and grain size subjected to uniaxial applied tension showed a peculiar size effect. The yield stress increased with diminishing film thickness, up to a thickness $h = 500\,\text{nm}$. Then, for $h = 300\,\text{nm}$, the yield stress appeared to have remained the same as for $h = 500\,\text{nm}$, indicating that the yield stress had attained a maximum value for $h \approx 400\,\text{nm}$. In another recent, similar experimental study [12], the yield stress of pure aluminum films increased up to a thickness $h = 100\,\text{nm}$; then, for $h < 100\,\text{nm}$, the yield stress started to decrease. This reversing (first hardening, then softening) size effect cannot be explained by any of the models proposed so far, because those models predict a hardening size effect (for constant grain size).

Here we model the film using continuum mechanics. We start by establishing expressions for the compressive stresses induced in the film by the surface stress. After adding these stresses to the applied stress, we use the von Mises yield condition to ascertain the value of the applied stress at initial yielding or *apparent yield stress*. Our results indicate that in films subjected to uniaxial applied tension the surface stress causes a reversing size effect on the apparent tensile yield stress. Based on

the values of surface stress determined in recent years via atomistic methods [13], we estimate that this size effect reverses for a thickness on the order of 100 nm, in accord with the experimental results summarized above.

Then, we use the well-known failure criterion proposed by Hancock and Mackenzie [14] to ascertain the mode of failure of the film. Our results indicate that the mode of failure changes from ductile to brittle for thicknesses close to the thickness for which the size effect reverses. These results are in accord with the experimental results of reference [11].

Last, we show that the surface stress may lead to entirely disparate size effects depending on the applied stress. In particular, we find that in films subjected to biaxial applied tension the surface stress does not lead to a reversing size effect. This finding reconciles the recent experimental results summarized above with J. W. Beams's experiments on gold and silver films, in which the size effect did not reverse even for $h = 20\,\text{nm}$ [15, 16].

Our work joins a growing body of research in which the surface stress has been found to play a crucial role in several problems at ultrasmall lengthscales, including the blunting of a crack tip [17] and the nanoindentation of a crystal [18].

2 Surface Stress

The surface stress is a second-rank tensor, $T_{\alpha\beta}$, where the indices α and β run from 1 to 2 and denote in-plane coordinates defined on the surface. (For detailed discussions of the surface stress see, for example, [19, 20].) To relate the surface stress to the surface energy, γ, using Eulerian coordinates [21], consider an element of surface of area A that is stretched by an in-plane *elastic* strain $\varepsilon_{\alpha\beta}$. Then, the work performed by the surface stress is $dW = AT_{\alpha\beta}\varepsilon_{\alpha\beta}$, and the energy of the element of surface, γA,

changes by $d(\gamma A) = \gamma dA + Ad\gamma = \gamma A\varepsilon_{\mu\mu} + A(\partial\gamma/\partial\varepsilon_{\alpha\beta})\varepsilon_{\alpha\beta}$, where repeated indices imply summation. Equating dW to $d(\gamma A)$ results in the desired expression for the surface stress, $T_{\alpha\beta} = \gamma\delta_{\alpha\beta} + \partial\gamma/\partial\varepsilon_{\alpha\beta}$, where $\delta_{\alpha\beta}$ is the second-rank Krönecker delta. The second term in the expression for $T_{\alpha\beta}$ represents the change in surface energy associated with the elastic stretching of the surface. When the area of a liquid surface is increased, the surface does not stretch elastically, because the atoms in the interior of the liquid are mobile and may readily migrate to the surface. Thus in liquids the second term in the expression for $T_{\alpha\beta}$ vanishes, and the surface stress is isotropic and equal to the surface energy. This is not the case in solids, because in solids the long-range order in the positions of the atoms makes it infeasible for the atoms to migrate to the surface, in particular when the strain applied to the surface amounts to a displacement of a small fraction of the lattice constant. Thus in solids the second term in the expression for $T_{\alpha\beta}$ may not necessarily vanish, and the surface stress is in general anisotropic.

Consider now the crystalline surface of a free-standing crystal. The surface accommodates the lattice constant of the bulk of the material by means of a spontaneous elastic stretching. If the crystalline surface possesses a threefold or higher rotational axial symmetry, then in the expression for $T_{\alpha\beta}$ the term $\partial\gamma/\partial\varepsilon_{\alpha\beta}$ associated with this elastic stretching is isotropic [13]. That is the case for (111) surfaces in FCC metals. In the experiments of interest here the films had a preferred $\langle 111\rangle$ crystallographic texture normal to the faces of the films, and we are justified in assuming an isotropic surface stress, $T_{\alpha\beta} = T\delta_{\alpha\beta}$. The surface stress may in principle be either positive (tensile) or negative, but it is positive for FCC metals.

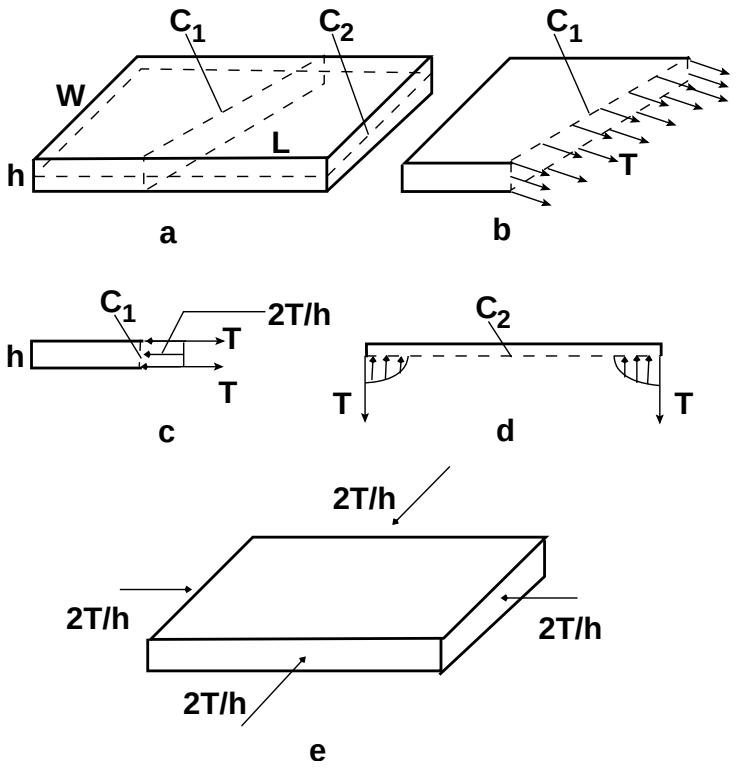

Figure 1: (a) A free-standing thin film. C_1 and C_2 are cuts performed for stress analysis. (b) The surface stress T acting on the perimeter of C_1. (c) The compressive stress induced by T on the surface of C_1. (d) The compressive stress induced by T on the surface of C_2. (e) Applied traction giving the same stresses as T.

3 The Surface Stress in Thin Films

Consider a free-standing film of length $L \gg h$ and width $W \gg h$ (Fig. 1a). Suppose that the film is severed through its thickness along an arbitrary in-plane direction. (The cut is marked C_1 in Fig. 1a.) Then, the surface stress, which we assume to be positive and isotropic, becomes manifest as a tensile force T per unit length of the perimeter of the cut, acting normal to the surface of the cut, as indicated in Fig. 1b. If the severed parts of the film are to remain in equilibrium, the surface stress must induce a compressive stress on the surface of the cut; because the film is very thin, the induced stress is uniform and of value $-2T/h$ on the surface of the cut (Fig. 1c). Thus the surface stress induces a compressive stress of value $-2T/h$ in all in-plane directions [19].

Suppose now that the film is severed parallel to its upper and lower faces. (The cut is marked C_2 in Fig. 1a.) Then, the surface stress must again induce a compressive stress on the surface of the cut, but now the stress is confined to a very narrow strip (of width $\sim h$) parallel to the lateral edges of the film, as indicated in Fig. 1d. Thus in most of the film the surface stress induces no stress in the direction of the thickness of the film.

From our discussion so far, we conclude that in a film of thickness h the stresses induced by the surface stress may be approximately simulated by (i) applying an in-plane compressive traction of value $-2T/h$ on all the lateral edges of the film and (ii) leaving the upper and lower faces of the film traction-free (Fig. 1e). This conclusion is valid where the film is thin, i.e., where $L \gg h$ and $W \gg h$.

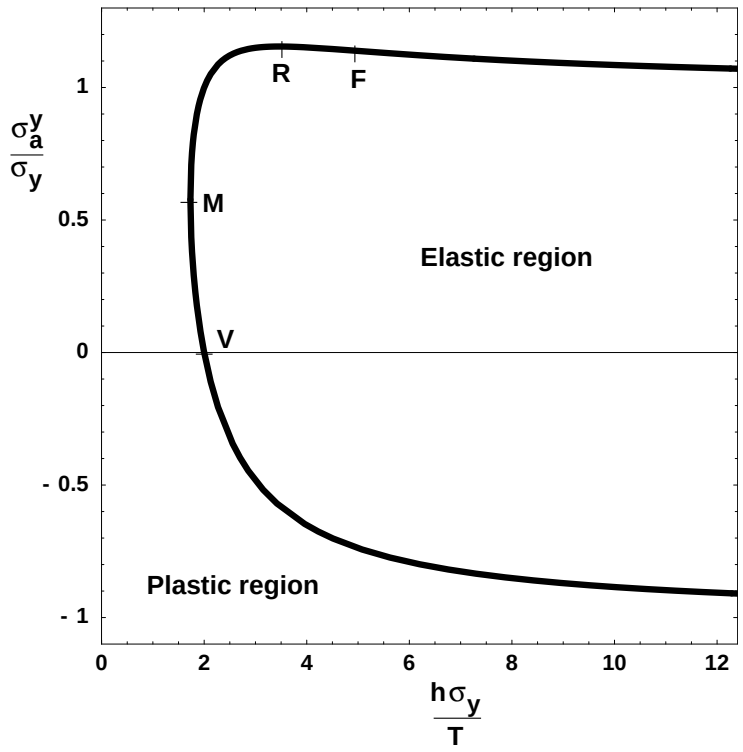

Figure 2: A plot of the dimensionless apparent yield stress σ_a^y/σ_y versus the dimensionless thickness $h\sigma_y/T$. See eq. (1). The points F, R, M, and V are referred to in the text. The size effect of the apparent tensile yield stress reverses from hardening to softening at the point R.

4 Apparent Yield Stress

Consider now a free-standing thin film to which a uniaxial stress σ_a is applied in the direction of the length of the film. Then, the film is uniformly subjected to principal stresses $\sigma_1 = \sigma_a - 2T/h$, $\sigma_2 = -2T/h$, and $\sigma_3 = 0$ in the direction of the length, the width, and the thickness, respectively. We may ascertain the value of the applied stress at initial yielding or *apparent yield stress*, σ_a^y, by substituting the principal stresses in the von Mises yield condition, $2\sigma_y^2 = (\sigma_1 - \sigma_2)^2 + (\sigma_2 - \sigma_3)^2 + (\sigma_3 - \sigma_1)^2$, where σ_y is the yield stress [22]. The result is

$$\frac{\sigma_a^y}{\sigma_y} = \frac{T}{h\sigma_y} \pm \sqrt{1 - 3\left(\frac{T}{h\sigma_y}\right)^2}. \tag{1}$$

Figure 2 shows a graphical rendition of (1) in the form of a plot of the dimensionless apparent yield stress, σ_a^y/σ_y, versus the dimensionless thickness, $h\sigma_y/T$. In the plot there is a single curve separating the elastic region (which the curve embraces) from the plastic region. The curve consists of two branches touching at their leftmost points (marked M in Fig. 2). The upper branch corresponds to the + sign in (1) and gives the apparent tensile yield stress. On the other hand, the lower branch corresponds to the − sign in (1) and gives the apparent compressive yield stress. The branches are supported on $h \geq h_M \equiv \sqrt{3}\,T/\sigma_y$ (because the discriminant of (1) is negative for $h < h_M$). Therefore, a film of thickness $h < h_M$ cannot be poised between the elastic region and the plastic region, regardless of the applied stress; such a film is always in the plastic region.

Figure 2 indicates that for $h \gg T/\sigma_y$ the apparent tensile yield stress is σ_y, and the apparent compressive yield stress $-\sigma_y$. Thus for $h \gg T/\sigma_y$ the initial yielding may be attained by applying a tensile stress σ_y or a compressive stress $-\sigma_y$. This is the expected asymptotic behavior.

Next, we discuss in turn the two branches of Fig. 2. Consider first the lower branch,

starting with a thin film of thickness $h \gg T/\sigma_y$. If the thickness of the film diminishes, the absolute value of the apparent compressive yield stress decreases (i.e., $d|\sigma_a^y|/dh < 0$), and we say that there is a softening size effect. If the thickness continues to diminish, then, for a thickness $h = h_V \equiv 2\,T/\sigma_y$, the apparent compressive yield stress vanishes, $\sigma_a^y = 0$ (point V in Fig. 2). Thus a free-standing film of thickness $h = h_V$ spontaneously attains the initial yielding by virtue of the compressive stresses induced by the surface stress. When a tensile stress is applied to this free-standing film, the film departs from the initial yielding, enters the elastic region, and re-attains the initial yielding at the apparent tensile yield stress given by the upper branch of Fig. 2. If the thickness continues to diminish beyond h_V, the apparent compressive yield stress becomes *positive* (i.e., the lower branch of Fig. 2 gives a *positive* value of σ_a^y). This positive value of σ_a^y is the minimum tensile stress that must be applied to the film if the film is not to yield by virtue of the *compressive* stresses induced by the surface stress. (Therefore, the name "apparent *compressive* yield stress" remains appropriate, even though this stress is positive.) Last, for a thickness $h = h_M \equiv \sqrt{3}\,T/\sigma_y$, we reach the leftmost point of the lower branch.

Consider now the upper branch of Fig. 2, starting with a thin film of thickness $h \gg T/\sigma_y$. If the thickness of the film diminishes, the apparent tensile yield stress increases (i.e., $d|\sigma_a^y|/dh < 0$), and we say that there is a hardening size effect. If the thickness of the film continues to diminish, then, for a thickness $h = h_F \approx 5\,T/\sigma_y$, the size effect is at its most hardening (i.e., $d^2|\sigma_a^y|/dh^2 = 0$; point F in Fig. 2). If the thickness continues to diminish beyond h_F, then the hardening size effect starts to lessen (i.e., $d|\sigma_a^y|/dh$ starts to become less negative). Eventually, for a thickness $h = h_R \equiv 2\sqrt{3}\,T/\sigma_y \approx 3.5\,T/\sigma_y$, the apparent tensile yield stress attains its maximum value, $\sigma_a^y = \sigma_{aR}^y \equiv 2\sigma_y/\sqrt{3} \approx 1.15\,\sigma_y$, and the size effect vanishes (i.e., $d|\sigma_a^y|/dh = 0$; point R in Fig. 2). If the thickness continues to diminish beyond h_R, the apparent tensile yield stress decreases (i.e., $d|\sigma_a^y|/dh > 0$), and we say that there is a softening size effect. Thus for a thickness $h = h_V \equiv 2\,T/\sigma_y$ the apparent tensile yield stress

equals its original value, $\sigma_a^y = \sigma_y$. Last, for a thickness $h = h_M \equiv \sqrt{3}\,T/\sigma_y \approx 1.73\,T/\sigma_y$, the apparent tensile yield stress equals its minimum value, $\sigma_a^y = \sigma_{aM}^y \equiv \sigma_y/\sqrt{3} \approx 0.58\,\sigma_y$, and we reach the leftmost point of the upper branch.

From our discussion of Fig. 2 we conclude that the surface stress causes a size effect on the apparent tensile yield stress. For thin films of thickness $h \gg T/\sigma_y$ there is a hardening size effect, but the size effect reverses from hardening to softening for a thickness $h_R \equiv 2\sqrt{3}\,T/\sigma_y$. Thus the stresses induced in a thin film by the surface stress lead to a size effect of the type recently observed in experiments.

5 Size Effects and the Yield Condition

We have predicated (1) on the von Mises yield condition, $\sigma_e = \sigma_y$. Here σ_e, the *equivalent stress*, quantifies the forcing that tends to produce plastic deformation; it is defined by the expression $2\sigma_e^2 \equiv (\sigma_1 - \sigma_2)^2 + (\sigma_2 - \sigma_3)^2 + (\sigma_3 - \sigma_1)^2$, where σ_1, σ_2, and σ_3 are the principal stresses. This expression for σ_e suitably quantifies the forcing if the plastic deformation occurs by the relative slip of adjacent planes in the material, regardless of the specific mechanisms whereby the slip is effected. (The slip need not be effected by dislocation motion, for example.) In fact, it is the yield stress, σ_y, and not the equivalent stress, σ_e, that depends on the specific mechanisms whereby the slip is effected. Thus the elucidation of size effects consists in determining the dependence of σ_y on the size. Yet this is not the case for the size effect caused by the surface stress, because this size effect is unrelated to the material. Instead, it is related to the stresses that act *on the bulk of the material* and to the fact that these stresses differ from the applied stresses. The elucidation of this size effect is not a problem in materials science, but rather a problem in solid mechanics.

In (1) the size effect caused by the surface stress is coupled to other size effects

only through the value of σ_y. Therefore, *in (1) the yield stress σ_y is not the yield stress of the bulk material, but the yield stress of the bulk material enhanced by any pertinent size effects other than the size effect caused by the surface stress.*

6 Comparison with Experiments

In Section 4, we concluded that the size effect caused by the surface stress reverses from hardening to softening for a thickness $h_R \equiv 2\sqrt{3}\,T/\sigma_y$. To compare the predicted value of h_R with the experimental results, we recall that for $h = h_R$ the (maximum) apparent tensile yield stress is $\sigma^y_{aR} \equiv 2\sigma_y/\sqrt{3}$, and write an expression for h_R in terms of σ^y_{aR}, with the result $h_R = 4T/\sigma^y_{aR}$.

(Note that $\sigma_y = \sigma^y_{aR}\sqrt{3}/2$ is the yield stress of the bulk material enhanced by any size effects other than the size effect caused by the surface stress; see Section 5. Note also that the expression $h_R = 4T/\sigma^y_{aR}$ can give only a rough estimate of the thickness for which the observed size effect reverses, not only because we have predicated this expression on a number of simplifying assumptions, but also because (a) the value of T may be strongly affected by subtle changes in environmental conditions and (b) σ^y_{aR} is difficult to measure, and tends to be overestimated both in experiments and in atomistic simulations; see, e.g., [23].)

For the pure gold films of the experimental study of reference [11], the reported maximum apparent tensile yield stress was $\sigma^y_{aR} = 170\,\text{MPa}$. Using the surface stress of gold given in reference [13] (see Appendix), $T = 3.41\,\text{N/m}$, we compute $h_R = 80\,\text{nm}$, which is on the order of magnitude of the thickness for which the observed size effect reversed in that study, $h \approx 400\,\text{nm}$.

For the pure aluminum thin films of the experimental study of reference [12], the reported *peak* stress was $\sigma^p_a = 750\,\text{MPa}$, and we estimate $\sigma^y_{aR} = \sigma^p_a/2 = 375\,\text{MPa}$.

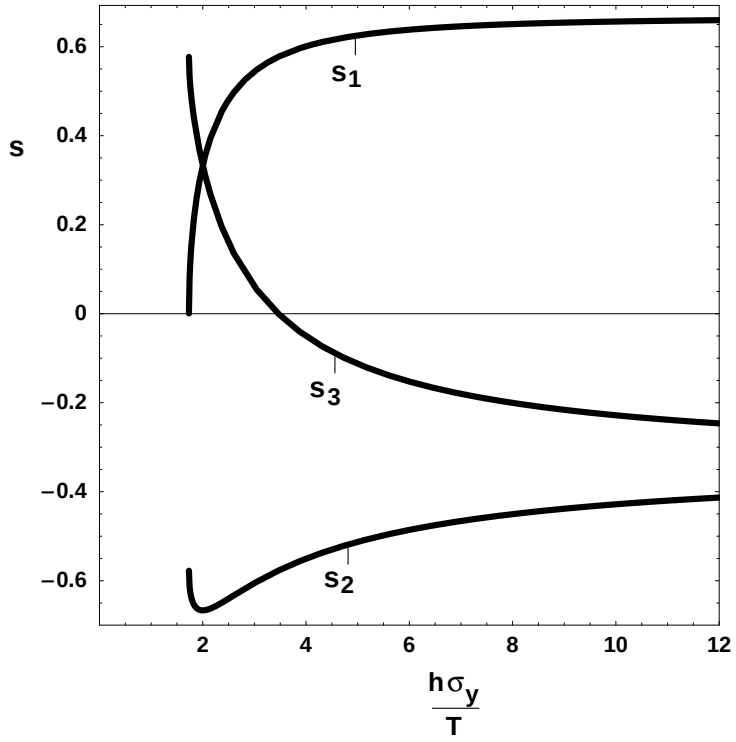

Figure 3: A plot of the dimensionless quantities s_1, s_2, and s_3 versus the dimensionless thickness, $h\sigma_y/T$. See eqs. (2–4).

Using the surface stress of aluminum given in reference [13] (see Appendix), $T = 2.29\,\mathrm{N/m}$, we compute $h_R = 24\,\mathrm{nm}$, which is on the order of magnitude of the thickness for which the observed size effect reversed in that study, $h \approx 100\,\mathrm{nm}$.

7 Failure and the Ductile-to-Brittle Transition

Upon attaining the initial yielding, the bulk of the film undergoes permanent deformation in the form of plastic strain increments $\Delta\varepsilon_1 = s_1\,\Delta\lambda$, $\Delta\varepsilon_2 = s_2\,\Delta\lambda$, and

$\Delta\varepsilon_3 = s_3\,\Delta\lambda$ in the direction of the length, the width, and the thickness of the film, respectively [22]. Here $\Delta\lambda$ is a dimensionless scalar factor, $s_1 = (\sigma_1 - p)/\sigma_y$, $s_2 = (\sigma_2 - p)/\sigma_y$, $s_3 = (\sigma_3 - p)/\sigma_y$, and $p = (\sigma_1 + \sigma_2 + \sigma_3)/3$. (Note that the plastic deformation is isochoric, $\Delta\varepsilon_1 + \Delta\varepsilon_2 + \Delta\varepsilon_3 = 0$.) By substituting $\sigma_1 = \sigma_a - 2T/h$, $\sigma_2 = -2T/h$, $\sigma_3 = 0$, and $\sigma_a = \sigma_a^y$ (where σ_a^y is the apparent tensile yield stress given by the upper branch of Fig. 2), we obtain

$$s_1 = \frac{2}{3}\sqrt{1 - 3\left(\frac{T}{h\sigma_y}\right)^2}, \tag{2}$$

$$s_2 = -\frac{T}{h\sigma_y} - \frac{1}{3}\sqrt{1 - 3\left(\frac{T}{h\sigma_y}\right)^2}, \quad \text{and} \tag{3}$$

$$s_3 = \frac{T}{h\sigma_y} - \frac{1}{3}\sqrt{1 - 3\left(\frac{T}{h\sigma_y}\right)^2}. \tag{4}$$

Figure 3 shows a graphical rendition of (2–4) in the form of plots of the dimensionless quantities s_1, s_2, and s_3 versus the dimensionless thickness, $h\sigma_y/T$. As was the case for Fig. 2, the plots in Fig. 3 are supported on $h \geq h_M \equiv \sqrt{3}\,T/\sigma_y$.

Consider now the process whereby the film accumulates plastic deformation, eventually leading to failure in the form of fracture. According to a well-known failure criterion [14], the onset of failure occurs when the *equivalent plastic strain*, ε_e, attains a critical value, ε_{ef}, that depends on the triaxiality of the stress in the form

$$\varepsilon_{ef} = \varepsilon_0 \exp\left(-p/\sigma_e\right), \tag{5}$$

where the subscript "f" stands for "at failure," ε_0 is a dimensionlesss constant, p/σ_e is a measure of the triaxiality of the stress, and the equivalent plastic strain is defined by the expression $9\,\varepsilon_e^2/2 = (\Delta\varepsilon_1 - \Delta\varepsilon_2)^2 + (\Delta\varepsilon_2 - \Delta\varepsilon_3)^2 + (\Delta\varepsilon_3 - \Delta\varepsilon_1)^2$. By evaluating ε_e with $\Delta\varepsilon_1 = s_1\,\Delta\lambda$, $\Delta\varepsilon_2 = s_2\,\Delta\lambda$, $\Delta\varepsilon_3 = s_3\,\Delta\lambda$, and the expressions for s_1, s_2, and s_3 given by (2–4), we obtain $\varepsilon_e = 2\,\Delta\lambda/3$; therefore, the value of $\Delta\lambda$ at failure is $\Delta\lambda_f = 3\,\varepsilon_{ef}/2$. On the other hand, by setting $\sigma_e = \sigma_y$ and evaluating p with

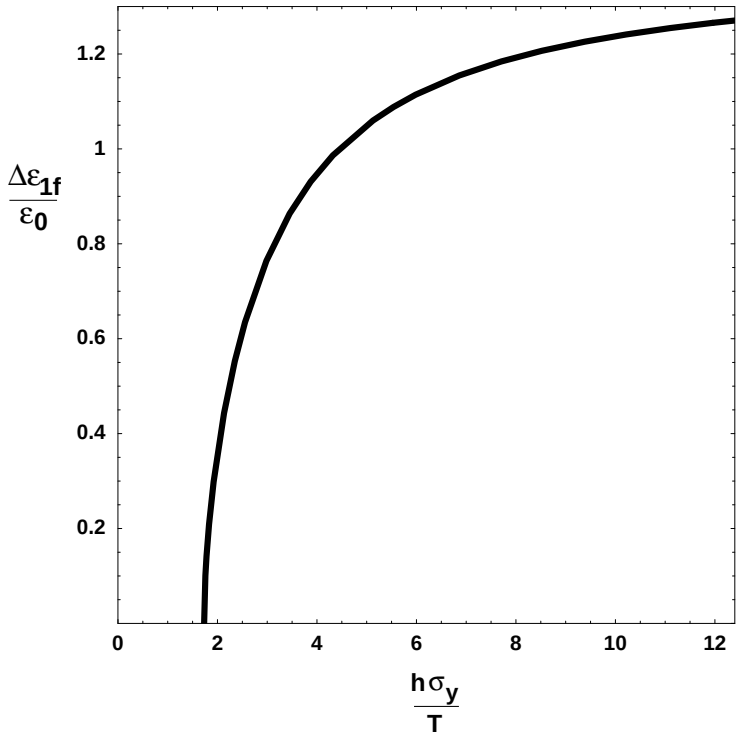

Figure 4: A plot of the normalized plastic strain at failure in the direction of the applied stress versus the dimensionless thickness, $h\sigma_y/T$. See eq. (6).

$\sigma_1 = \sigma_a - 2T/h$, $\sigma_2 = -2T/h$, $\sigma_3 = 0$, and $\sigma_a = \sigma_a^y$ (where σ_a^y is the apparent tensile yield stress given by the upper branch of Fig. 2), we obtain $p/\sigma_e = s_3$. Since $\Delta\lambda_f = 3\,\varepsilon_{ef}/2$ and $p/\sigma_e = s_3$, we can recast (5) in the form $\Delta\lambda_f = (3/2)\,\varepsilon_0 \exp(-s_3)$, and write an expression for the plastic strain at failure *in the direction of the applied stress*, $\Delta\varepsilon_{1f}$, as follows:

$$\Delta\varepsilon_{1f} = (3/2)\,\varepsilon_0\, s_1 \exp(-s_3). \tag{6}$$

Fig. 4 shows a graphical rendition of (6) in the form a plot of $\Delta\varepsilon_{1f}/\varepsilon_0$ versus the dimensionless thickness, $h\sigma_y/T$. From the plot in Fig. 4, we conclude that the plastic strain at failure in the direction of the applied stress diminishes as the film becomes thinner. (Note that $\Delta\varepsilon_{1f}$ diminishes due to the combined effect of a lessening of s_1 and an increase in triaxiality.) In other words, the failure becomes increasingly brittle as the film becomes thinner. Further, the rate of embrittlement becomes very strong for thicknesses close to the thickness for which the size effect reverses, $h_R = 2\sqrt{3}\,T/\sigma_y$.

Our conlusions from the previous paragraph are in accord with the results of recent experiments on gold films [11], in which a ductile-to-brittle transition was documented for a thickness on the order of 100 nm.

8 Biaxial Loading

To inquire further into the size effect caused by the surface stress, we now consider a type of experiment known as the *bulge test*. In the bulge test, a film of thickness h is placed across the open end of a circular tube of radius $R \gg h$. Then, the pressure of the air in the tube is increased to a value p, whereupon the film deflects to form a bulge of height $b \ll R$. As a result, the film is subjected to a *biaxial*, in-plane isotropic applied stress $\sigma_a = pR^2/4bh \gg p$. In a classic experimental study, J. W. Beams used the bulge test to determine the apparent yield stress of polycrystalline gold and silver

films of thicknesses in the range of 200 to 20 nm [15, 16]. He concluded that the apparent yield stress increased monotonically with diminishing film thickness. Thus, in contrast with the recent experimental studies summarized above, a reversing size effect was *not* observed in Beam's classical experimental study.

To understand this discrepancy, we substitute the principal stresses of the bulge test ($\sigma_1 = \sigma_a - 2T/h$, $\sigma_2 = \sigma_a - 2T/h$, and $\sigma_3 = 0$) in the von Mises yield condition, with the result

$$\frac{\sigma_a^y}{\sigma_y} = \pm 1 + 2\frac{T}{h\sigma_y}, \tag{7}$$

where σ_a^y is the apparent yield stress [24]. Equation (7) predicts a hardening size effect in the apparent tensile yield stress measured in bulge tests, as expected. In a 1959 review paper [16], Beams is said to have first ascribed the hardening size effect observed in his experiments to the surface *energy*. In the same paper, a plot is shown and attributed to Beams which might be a graphical rendition of (7). Unfortunately, Beams appears not to have published the equations leading to this plot. (He subsequently came to the conclusion that the size effect observed in his experiments could not be ascribed to the surface energy, because for relatively thick thin films the predicted size effect fell short of the observed size effect [16]. It was thought at the time that the observed size effect should be ascribed to a *single* reason.)

From our discussion of the bulge test we conclude that, in contrast with our results for thin films subjected to a uniaxial applied stress, the surface stress does not lead to a reversing size effect in thin films subjected to a biaxial, isotropic applied stress.

9 Discussion

We have concluded that in ultrathin, polycrystalline metallic films the surface stress leads to a size effect in the initial yielding that depends strongly on the applied

stress, in accord with experiments. Where the applied stress is uniaxial, the size effect reverses for a film thickness h_R that can be estimated using values of the surface stress determined via atomistic methods. The result, $h_R \approx 100\,\mathrm{nm}$, is in accord with experiments. In addtion, we have predicted that the mode of failure of the film changes from ductile to brittle for thicknesses close to h_R, also in accord with experiments.

To reach these conclusions, we have used continuum mechanics. Given that the film thickness for which the size effect reverses is only about 100 times a typical lattice parameter, our conclusions add to a growing realization of the robustness of continuum mechanics at ultrasmall lengthscales, a realization that has been commented upon by a number of authors. (For a recent, eloquent example from the field of microfluidics see [25].)

We thank Prof. K. Jimmy Hsia for a number of discussions and for his encouragement in the course of this research. Prof. James W. Phillips kindly read our manuscript and suggested ways of improving it.

References

[1] Bažant, Z. P., and Chen, E. P., 1997, "Scaling of Structural Failure," Appl. Mech. Reviews, **10**, pp. 593–527.

[2] Brenner, S. S., 1956, "Tensile Strength of Whiskers," J. Applied Phys., **27**, pp. 1484–1491.

[3] Fleck, N. A., Muller, G. M., Ashby, M. F., Hutchinson, J. W., 1994, "Strain Gradient Plasticity: Theory and Experiment," Acta Metall. Mater., **42**, pp. 475–487.

[4] Fleck, N. A., and Hutchinson, J. W., 1997, "Strain Gradient Plasticity," Adv. Appl. Mech., **33**, pp. 295–261.

[5] Lejeck P., and Sima, V., 1983, "Orientational Relationships in the Secondary Recrystallization of Pure Nickel," Mater. Sci. Eng., **60**, pp. 121–124.

[6] Grant, E. M., Hansen, N., Jensen, D. J., Ralph, B., Stobbs, W. M., 1988, "Texture Development During Grain Growth in Thin Films," in *Proceedings of the Eighth International Conference on Texture of Materials*, edited by Kallend, J. S., and Gottstein, G. (Springer-Verlag, New York).

[7] Griffin, A. J., Brotzen, F. R., and Dunn, C. F., 1987, "Mechanical-Properties and Microstructures of Al-1-Percent-Si Thin-Film Metallizations," Thin Solid Films **150**, pp. 237–244.

[8] Venkatraman, R., and Bravman, J. C., 1992, "Separation of Film Thickness and Grain Boundary Strengthening Effects in Al Thin Films on Si," J. Mater. Res. **7**, pp. 2040–2048.

[9] Thompson, C. V., 1993, "The Yield Stress of Polycrytalline Thin Films," J. Mater. Res., **8**, pp. 237–238.

[10] Schiotz, J. and Jacobsen, K. W., 2003, "A Maximum in the Strength of Nanocrystalline Copper," Science, **301**, pp. 1357–1359.

[11] Espinosa, H. D., Prorok, B. C., and Peng, B., 2004, "Plasticity Size Effects in Free-Standing Submicron Polycrystalline FCC Films Subjected to Pure Tension," J. Mech. Phys. Solids, **52**, pp. 667–689.

[12] Saif, T., 2004, "Scaling the Depths," Mech. Engr., **126**, pp. 8–11. See also Haque, A., 2002, "Length-Scale Effects on Nano-Scale Materials Behavior," PhD Thesis, Department of Mechanical Engineering, University of Illinois at Urbana-Champaign.

[13] Wan, J., Fan, Y. L., Gong, D. W., Shen, S .G., and Fan, X. Q., 1999, " Surface Relaxation and Stress of FCC Metals: Cu, Ag, Au, Ni, Pd, Pt, Al and Pb," Modelling Simul. Matr. Sci. Eng., **7**, pp. 189–206.

[14] Hancock, J. W., Mackenzie, A. C., 1976, "On the Mechanisms of Ductile Failure in High-Strength Steels Subjected to Multi-Axial Stress States," J. Mech. Phys. Solids, **24**, pp. 147–169.

[15] Beams, J. W., 1959, "Mechanical Properties of Thin Films of Gold and Silver," in *Structure and Properties of Thin Films*, edited by Neugebauer, C. A., Newkirk, C. A., and Vermilyea, D. A. (John Willey & Sons, New York), pp. 183–198.

[16] Menter, J. W. and Pashley, D. W., 1959, "The Microstructure and Mechanical Properties of Thin Films," in *Structure and Properties of Thin Films*, edited by Neugebauer, C. A., Newkirk, C. A., and Vermilyea, D. A. (John Willey & Sons, New York), pp. 111–150.

[17] Carlsson, A. E. and Thomson, R., 1988, "Fracture Toughness of Materials: From Atomistics to Continuum Theory," Solid State Phys., **51**, pp. 233–280.

[18] Knap, J. and Ortiz, M., 2003, "Effect of Indenter-Radius Size on Au(001) Nanoindentation," Phys. Rev. Lett., **90**, 226102.

[19] Herring, C., 1953, in *Structure and Properties of Solid Surfaces*, edited by Gomer, R. and Smith, C. S. (The University of Chicago Press).

[20] Cammarata, R. C., 1994, "Surface and Interface Stress Effects in Thin-Films," Prog. Surf. Sci., **46**, pp. 1–38.

[21] Nix, W. D. and Gao, H., 1998, "An Atomistic Interpretation of Interface Stress," Scripta Mater., **39**, pp. 1653–1661.

[22] Calladine, C. R., *Plasticity* (Horwood Publishing Ltd., Chichester, UK, 2000), p. 48.

[23] Schiotz, J., Vegge, T., Di Tolla, F. D., and Jacobsen, K. W., 1999, "Atomic-scale Simulations of the Mechanical Deformation on Nanocrystalline Metals," Phys. Rev. B, **60**, pp. 11971–11983.

[24] It is straightforward to show that this same size effect is valid for wires. For atomistic simulations in ultrathin wires, see, for example, Gall, K., Diao, J., and Dunn, M. L., 2004, "The Strength of Gold Nanowires," Nanoletters, **4**, pp. 2431–2436.

[25] Sharp, K. V., and Adrian R. J., 2004, "Transition from Laminar to Turbulent Flow in Liquid Filled Microtubes," Exp. Fluids, **36**, pp. 741–747.

Appendix

In the calculations of Section 6 we use the (111) unrelaxed surface stress computed by the modified embedded atom method and reported in [13]. (In this useful reference, the surface stresses and surface energies obtained by a number of methods are given for all FCC metals: Cu, Ag, Au, Ni, Pd, Pt, Al, and Pb. Different methods lead to comparable results, and the results are in good agreement with the few available experimental measurements.) Note that this surface stress corresponds to a free-standing crystal and does not account for the additional elastic stretching undergone by the surface (as well as by the bulk of the material) as the film is stressed to the initial yielding. The required correction is negligible, however. In fact, a straightforward application of the atomistic model of Nix and Gao [21] allows us to estimate the required correction as $\Delta T \approx 2E\varepsilon a$, where E is the Young's modulus, ε is the strain associated with the additional elastic stretching, and a is the lattice constant;

for gold we use $E\varepsilon = \sigma_y = 170\,\mathrm{MPa}$ and $a = 0.3\,\mathrm{nm}$, with the result $\Delta T \approx 0.11\,\mathrm{N/m} \ll T = 3.41\,\mathrm{N/m}$.

Note also that a small increment in the *plastic* deformation brings additional atoms to the surface of the film but does not cause an additional elastic stretching of the surface (or of the bulk of the material) [21]. We conclude that the area of the surface of a film may change as a result of a small increment in plastic deformation, but the surface retains the same structure and remains equally stretched, so that the energy of the surface changes by TdA, where T is the surface stress of the free-standing film, and dA is the change in surface area. As an example of application of this conclusion, consider a film that undergoes plastic strain increments $d\varepsilon_1$, $d\varepsilon_2$, and $d\varepsilon_3$ in the direction of L, W, and h, respectively, where $d\varepsilon_3 = -(d\varepsilon_1 + d\varepsilon_2)$. The energy of the surface changes by $dW_s = TdA = T\left(2LW(d\varepsilon_1 + d\varepsilon_2) + 2(L+W)hd\varepsilon_3\right) = 2T\left(LW - (L+W)h\right)(d\varepsilon_1 + d\varepsilon_2)$, the stresses in the bulk of the film perform a plastic work $dW_p = (\sigma_1 d\varepsilon_1 + \sigma_2 d\varepsilon_2 + \sigma_3 d\varepsilon_3)LWh$, and the applied traction performs a work $dW_a = \sigma_a LWhd\varepsilon_1$. Equating $dW_a = dW_s + dW_p$ leads to $\sigma_1 = \sigma_a - 2T/h\left(1 - (1 + L/W)h/L\right)$, $\sigma_2 = -2T/h\left(1 - (1 + L/W)h/L\right)$, and $\sigma_3 = 0$, which under the assumption $h/L \ll 1$ simplifies to $\sigma_1 = \sigma_a - 2T/h$, $\sigma_2 = -2T/h$, and $\sigma_3 = 0$, as we concluded before under the same assumption.

List of Recent TAM Reports

No.	Authors	Title	Date
987	Phillips, W. R. C.	Langmuir circulations—*Surface Waves* (J. C. R. Hunt and S. Sajjadi, eds.), in press (2002)	Nov. 2001
988	Gioia, G., and F. A. Bombardelli	Scaling and similarity in rough channel flows—*Physical Review Letters* **88**, 014501 (2002)	Nov. 2001
989	Riahi, D. N.	On stationary and oscillatory modes of flow instabilities in a rotating porous layer during alloy solidification—*Journal of Porous Media* **6**, 1–11 (2003)	Nov. 2001
990	Okhuysen, B. S., and D. N. Riahi	Effect of Coriolis force on instabilities of liquid and mushy regions during alloy solidification—*Physics of Fluids* (submitted)	Dec. 2001
991	Christensen, K. T., and R. J. Adrian	Measurement of instantaneous Eulerian acceleration fields by particle-image accelerometry: Method and accuracy—*Experimental Fluids* (submitted)	Dec. 2001
992	Liu, M., and K. J. Hsia	Interfacial cracks between piezoelectric and elastic materials under in-plane electric loading—*Journal of the Mechanics and Physics of Solids* **51**, 921–944 (2003)	Dec. 2001
993	Panat, R. P., S. Zhang, and K. J. Hsia	Bond coat surface rumpling in thermal barrier coatings—*Acta Materialia* **51**, 239–249 (2003)	Jan. 2002
994	Aref, H.	A transformation of the point vortex equations—*Physics of Fluids* **14**, 2395–2401 (2002)	Jan. 2002
995	Saif, M. T. A, S. Zhang, A. Haque, and K. J. Hsia	Effect of native Al_2O_3 on the elastic response of nanoscale aluminum films—*Acta Materialia* **50**, 2779–2786 (2002)	Jan. 2002
996	Fried, E., and M. E. Gurtin	A nonequilibrium theory of epitaxial growth that accounts for surface stress and surface diffusion—*Journal of the Mechanics and Physics of Solids* **51**, 487–517 (2003)	Jan. 2002
997	Aref, H.	The development of chaotic advection—*Physics of Fluids* **14**, 1315–1325 (2002); see also *Virtual Journal of Nanoscale Science and Technology*, 11 March 2002	Jan. 2002
998	Christensen, K. T., and R. J. Adrian	The velocity and acceleration signatures of small-scale vortices in turbulent channel flow—*Journal of Turbulence*, in press (2002)	Jan. 2002
999	Riahi, D. N.	Flow instabilities in a horizontal dendrite layer rotating about an inclined axis—*Journal of Porous Media*, in press (2003)	Feb. 2002
1000	Kessler, M. R., and S. R. White	Cure kinetics of ring-opening metathesis polymerization of dicyclopentadiene—*Journal of Polymer Science A* **40**, 2373–2383 (2002)	Feb. 2002
1001	Dolbow, J. E., E. Fried, and A. Q. Shen	Point defects in nematic gels: The case for hedgehogs—*Archive for Rational Mechanics and Analysis* **177**, 21–51 (2005)	Feb. 2002
1002	Riahi, D. N.	Nonlinear steady convection in rotating mushy layers—*Journal of Fluid Mechanics* **485**, 279–306 (2003)	Mar. 2002
1003	Carlson, D. E., E. Fried, and S. Sellers	The totality of soft-states in a neo-classical nematic elastomer—*Journal of Elasticity* **69**, 169–180 (2003) with revised title	Mar. 2002
1004	Fried, E., and R. E. Todres	Normal-stress differences and the detection of disclinations in nematic elastomers—*Journal of Polymer Science B: Polymer Physics* **40**, 2098–2106 (2002)	June 2002
1005	Fried, E., and B. C. Roy	Gravity-induced segregation of cohesionless granular mixtures—*Lecture Notes in Mechanics*, in press (2002)	July 2002
1006	Tomkins, C. D., and R. J. Adrian	Spanwise structure and scale growth in turbulent boundary layers—*Journal of Fluid Mechanics* (submitted)	Aug. 2002
1007	Riahi, D. N.	On nonlinear convection in mushy layers: Part 2. Mixed oscillatory and stationary modes of convection—*Journal of Fluid Mechanics* **517**, 71–102 (2004)	Sept. 2002
1008	Aref, H., P. K. Newton, M. A. Stremler, T. Tokieda, and D. L. Vainchtein	Vortex crystals—*Advances in Applied Mathematics* **39**, in press (2002)	Oct. 2002

List of Recent TAM Reports (cont'd)

No.	*Authors*	*Title*	*Date*
1009	Bagchi, P., and S. Balachandar	Effect of turbulence on the drag and lift of a particle—*Physics of Fluids*, in press (2003)	Oct. 2002
1010	Zhang, S., R. Panat, and K. J. Hsia	Influence of surface morphology on the adhesive strength of aluminum/epoxy interfaces—*Journal of Adhesion Science and Technology* **17**, 1685–1711 (2003)	Oct. 2002
1011	Carlson, D. E., E. Fried, and D. A. Tortorelli	On internal constraints in continuum mechanics—*Journal of Elasticity* **70**, 101–109 (2003)	Oct. 2002
1012	Boyland, P. L., M. A. Stremler, and H. Aref	Topological fluid mechanics of point vortex motions—*Physica D* **175**, 69–95 (2002)	Oct. 2002
1013	Bhattacharjee, P., and D. N. Riahi	Computational studies of the effect of rotation on convection during protein crystallization—*International Journal of Mathematical Sciences*, in press (2004)	Feb. 2003
1014	Brown, E. N., M. R. Kessler, N. R. Sottos, and S. R. White	*In situ* poly(urea-formaldehyde) microencapsulation of dicyclopentadiene—*Journal of Microencapsulation* (submitted)	Feb. 2003
1015	Brown, E. N., S. R. White, and N. R. Sottos	Microcapsule induced toughening in a self-healing polymer composite—*Journal of Materials Science* (submitted)	Feb. 2003
1016	Kuznetsov, I. R., and D. S. Stewart	Burning rate of energetic materials with thermal expansion—*Combustion and Flame* (submitted)	Mar. 2003
1017	Dolbow, J., E. Fried, and H. Ji	Chemically induced swelling of hydrogels—*Journal of the Mechanics and Physics of Solids*, in press (2003)	Mar. 2003
1018	Costello, G. A.	Mechanics of wire rope—Mordica Lecture, Interwire 2003, Wire Association International, Atlanta, Georgia, May 12, 2003	Mar. 2003
1019	Wang, J., N. R. Sottos, and R. L. Weaver	Thin film adhesion measurement by laser induced stress waves—*Journal of the Mechanics and Physics of Solids* (submitted)	Apr. 2003
1020	Bhattacharjee, P., and D. N. Riahi	Effect of rotation on surface tension driven flow during protein crystallization—*Microgravity Science and Technology* **14**, 36–44 (2003)	Apr. 2003
1021	Fried, E.	The configurational and standard force balances are not always statements of a single law—*Proceedings of the Royal Society* (submitted)	Apr. 2003
1022	Panat, R. P., and K. J. Hsia	Experimental investigation of the bond coat rumpling instability under isothermal and cyclic thermal histories in thermal barrier systems—*Proceedings of the Royal Society of London A* **460**, 1957–1979 (2003)	May 2003
1023	Fried, E., and M. E. Gurtin	A unified treatment of evolving interfaces accounting for small deformations and atomic transport: grain-boundaries, phase transitions, epitaxy—*Advances in Applied Mechanics* **40**, 1–177 (2004)	May 2003
1024	Dong, F., D. N. Riahi, and A. T. Hsui	On similarity waves in compacting media—*Horizons in World Physics* **244**, 45–82 (2004)	May 2003
1025	Liu, M., and K. J. Hsia	Locking of electric field induced non-180° domain switching and phase transition in ferroelectric materials upon cyclic electric fatigue—*Applied Physics Letters* **83**, 3978–3980 (2003)	May 2003
1026	Liu, M., K. J. Hsia, and M. Sardela Jr.	In situ X-ray diffraction study of electric field induced domain switching and phase transition in PZT-5H—*Journal of the American Ceramics Society* (submitted)	May 2003
1027	Riahi, D. N.	On flow of binary alloys during crystal growth—*Recent Research Development in Crystal Growth*, in press (2003)	May 2003
1028	Riahi, D. N.	On fluid dynamics during crystallization—*Recent Research Development in Fluid Dynamics*, in press (2003)	July 2003
1029	Fried, E., V. Korchagin, and R. E. Todres	Biaxial disclinated states in nematic elastomers—*Journal of Chemical Physics* **119**, 13170–13179 (2003)	July 2003
1030	Sharp, K. V., and R. J. Adrian	Transition from laminar to turbulent flow in liquid filled microtubes—*Physics of Fluids* (submitted)	July 2003

List of Recent TAM Reports (cont'd)

No.	*Authors*	*Title*	*Date*
1031	Yoon, H. S., D. F. Hill, S. Balachandar, R. J. Adrian, and M. Y. Ha	Reynolds number scaling of flow in a Rushton turbine stirred tank: Part I—Mean flow, circular jet and tip vortex scaling—*Chemical Engineering Science* (submitted)	Aug. 2003
1032	Raju, R., S. Balachandar, D. F. Hill, and R. J. Adrian	Reynolds number scaling of flow in a Rushton turbine stirred tank: Part II—Eigen-decomposition of fluctuation—*Chemical Engineering Science* (submitted)	Aug. 2003
1033	Hill, K. M., G. Gioia, and V. V. Tota	Structure and kinematics in dense free-surface granular flow—*Physical Review Letters* **91**, 064302 (2003)	Aug. 2003
1034	Fried, E., and S. Sellers	Free-energy density functions for nematic elastomers—*Journal of the Mechanics and Physics of Solids* **52**, 1671–1689 (2004)	Sept. 2003
1035	Kasimov, A. R., and D. S. Stewart	On the dynamics of self-sustained one-dimensional detonations: A numerical study in the shock-attached frame—*Physics of Fluids* (submitted)	Nov. 2003
1036	Fried, E., and B. C. Roy	Disclinations in a homogeneously deformed nematic elastomer—*Nature Materials* (submitted)	Nov. 2003
1037	Fried, E., and M. E. Gurtin	The unifying nature of the configurational force balance—*Mechanics of Material Forces* (P. Steinmann and G. A. Maugin, eds.), in press (2003)	Dec. 2003
1038	Panat, R., K. J. Hsia, and J. W. Oldham	Rumpling instability in thermal barrier systems under isothermal conditions in vacuum—*Philosophical Magazine*, in press (2004)	Dec. 2003
1039	Cermelli, P., E. Fried, and M. E. Gurtin	Sharp-interface nematic–isotropic phase transitions without flow—*Archive for Rational Mechanics and Analysis* **174**, 151–178 (2004)	Dec. 2003
1040	Yoo, S., and D. S. Stewart	A hybrid level-set method in two and three dimensions for modeling detonation and combustion problems in complex geometries—*Combustion Theory and Modeling* (submitted)	Feb. 2004
1041	Dienberg, C. E., S. E. Ott-Monsivais, J. L. Ranchero, A. A. Rzeszutko, and C. L. Winter	Proceedings of the Fifth Annual Research Conference in Mechanics (April 2003), TAM Department, UIUC (E. N. Brown, ed.)	Feb. 2004
1042	Kasimov, A. R., and D. S. Stewart	Asymptotic theory of ignition and failure of self-sustained detonations—*Journal of Fluid Mechanics* (submitted)	Feb. 2004
1043	Kasimov, A. R., and D. S. Stewart	Theory of direct initiation of gaseous detonations and comparison with experiment—*Proceedings of the Combustion Institute* (submitted)	Mar. 2004
1044	Panat, R., K. J. Hsia, and D. G. Cahill	Evolution of surface waviness in thin films via volume and surface diffusion—*Journal of Applied Physics* (submitted)	Mar. 2004
1045	Riahi, D. N.	Steady and oscillatory flow in a mushy layer—*Current Topics in Crystal Growth Research*, in press (2004)	Mar. 2004
1046	Riahi, D. N.	Modeling flows in protein crystal growth—*Current Topics in Crystal Growth Research*, in press (2004)	Mar. 2004
1047	Bagchi, P., and S. Balachandar	Response of the wake of an isolated particle to isotropic turbulent cross-flow—*Journal of Fluid Mechanics* (submitted)	Mar. 2004
1048	Brown, E. N., S. R. White, and N. R. Sottos	Fatigue crack propagation in microcapsule toughened epoxy—*Journal of Materials Science* (submitted)	Apr. 2004
1049	Zeng, L., S. Balachandar, and P. Fischer	Wall-induced forces on a rigid sphere at finite Reynolds number—*Journal of Fluid Mechanics* (submitted)	May 2004
1050	Dolbow, J., E. Fried, and H. Ji	A numerical strategy for investigating the kinetic response of stimulus-responsive hydrogels—*Computer Methods in Applied Mechanics and Engineering* **194**, 4447–4480 (2005)	June 2004
1051	Riahi, D. N.	Effect of permeability on steady flow in a dendrite layer—*Journal of Porous Media*, in press (2004)	July 2004

List of Recent TAM Reports (cont'd)

No.	*Authors*	*Title*	*Date*
1052	Cermelli, P., E. Fried, and M. E. Gurtin	Transport relations for surface integrals arising in the formulation of balance laws for evolving fluid interfaces—*Journal of Fluid Mechanics* (submitted)	Sept. 2004
1053	Stewart, D. S., and A. R. Kasimov	Theory of detonation with an embedded sonic locus—*SIAM Journal on Applied Mathematics* (submitted)	Oct. 2004
1054	Stewart, D. S., K. C. Tang, S. Yoo, M. Q. Brewster, and I. R. Kuznetsov	Multi-scale modeling of solid rocket motors: Time integration methods from computational aerodynamics applied to stable quasi-steady motor burning—*Proceedings of the 43rd AIAA Aerospace Sciences Meeting and Exhibit* (January 2005), Paper AIAA-2005-0357 (2005)	Oct. 2004
1055	Ji, H., H. Mourad, E. Fried, and J. Dolbow	Kinetics of thermally induced swelling of hydrogels—*International Journal of Solids and Structures* (submitted)	Dec. 2004
1056	Fulton, J. M., S. Hussain, J. H. Lai, M. E. Ly, S. A. McGough, G. M. Miller, R. Oats, L. A. Shipton, P. K. Shreeman, D. S. Widrevitz, and E. A. Zimmermann	Final reports: Mechanics of complex materials, Summer 2004 (K. M. Hill and J. W. Phillips, eds.)	Dec. 2004
1057	Hill, K. M., G. Gioia, and D. R. Amaravadi	Radial segregation patterns in rotating granular mixtures: Waviness selection—*Physical Review Letters* **93**, 224301 (2004)	Dec. 2004
1058	Riahi, D. N.	Nonlinear oscillatory convection in rotating mushy layers—*Journal of Fluid Mechanics* (submitted)	Dec. 2004
1059	Okhuysen, B. S., and D. N. Riahi	On buoyant convection in binary solidification—*Journal of Fluid Mechanics* (submitted)	Jan. 2005
1060	Brown, E. N., S. R. White, and N. R. Sottos	Retardation and repair of fatigue cracks in a microcapsule toughened epoxy composite—Part I: Manual infiltration—*Composites Science and Technology* (submitted)	Jan. 2005
1061	Brown, E. N., S. R. White, and N. R. Sottos	Retardation and repair of fatigue cracks in a microcapsule toughened epoxy composite—Part II: *In situ* self-healing—*Composites Science and Technology* (submitted)	Jan. 2005
1062	Berfield, T. A., R. J. Ong, D. A. Payne, and N. R. Sottos	Residual stress effects on piezoelectric response of sol-gel derived PZT thin films—*Journal of Applied Physics* (submitted)	Apr. 2005
1063	Anderson, D. M., P. Cermelli, E. Fried, M. E. Gurtin, and G. B. McFadden	General dynamical sharp-interface conditions for phase transformations in viscous heat-conducting fluids—*Journal of Fluid Mechanics* (submitted)	Apr. 2005
1064	Fried, E., and M. E. Gurtin	Second-gradient fluids: A theory for incompressible flows at small length scales—*Journal of Fluid Mechanics* (submitted)	Apr. 2005
1065	Gioia, G., and F. A. Bombardelli	Localized turbulent flows on scouring granular beds—*Physical Review Letters*, in press (2005)	May 2005
1066	Fried, E., and S. Sellers	Orientational order and finite strain in nematic elastomers—*Journal of Chemical Physics* **123**, 044901 (2005)	May 2005
1067	Chen, Y.-C., and E. Fried	Uniaxial nematic elastomers: Constitutive framework and a simple application—*Proceedings of the Royal Society of London A* (submitted)	June 2005
1068	Fried, E., and S. Sellers	Incompatible strains associated with defects in nematic elastomers—*Physical Review Letters* (submitted)	Aug. 2005
1069	Gioia, G., and X. Dai	Surface stress and reversing size effect in the initial yielding of ultrathin films—*Journal of Applied Mechanics*, in press (2005)	Aug. 2005
1070	Gioia, G., and P. Chakraborty	Turbulent friction in rough pipes and the energy spectrum of the phenomenological theory—*arXiv:physics* 0507066 v1 8 Jul 2005	Aug. 2005